Comparison of the Cation Valence and Coordination in Ce_2UO_6 and Ce_2MoO_6

Mark R. Antonio,* U. Staub, J. S. Xue, and L. Soderholm*

Chemistry Division, Argonne National Laboratory, Argonne, Illinois 60439-4831

Received March 29, 1996. Revised Manuscript Received July 16, 1996[⊗]

Ce_2UO_6 and Ce_2MoO_6 have both been suggested to have significant charge transfer between the metal ions. To quantify this proposed charge transfer, the valence and coordination of cerium and uranium in Ce_2UO_6 as well as cerium and molybdenum in Ce_2MoO_6 were studied through a combination of K-, L-, and M-edge XAFS (X-ray absorption fine structure). The results clearly show that these two compounds are not isostructural. Whereas Ce and U in Ce_2UO_6 are found to disorder on a single site, consistent with the formation of the solid solution $Ce_{0.67}U_{0.33}O_2$, the Ce and Mo coordination is very different. The Mo sits on a site with tetrahedral coordination. The XANES (X-ray absorption near edge structure) data show that for Ce_2UO_6, Ce and U are both tetravalent, whereas for Ce_2MoO_6, Ce is trivalent and Mo is hexavalent. There is no evidence in either compound for any significant charge transfer or intermediate valence. The unusual physical properties exhibited by these materials are discussed in light of these findings.

Introduction

Compounds that contain metal ions with variable oxidation states sometimes exhibit unusual charge-transfer and conductivity properties that may be of theoretical interest and technological importance. In particular, interesting properties arise in mixed-metal oxides containing both a rare-earth and a transition-metal ion in which the chemical potential of the f ion is energetically close to the Fermi level of the bands formed from the transition-metal d states. In situ charge transfer can occur and, depending on its time scale, can result in intermediate-valent or heavy-fermion behavior[1−3] or selective catalytic activity.[4,5] Usually these types of behaviors are found when the f ion is a light lanthanide or actinide, notably Ce or U. This is thought to be because Ce and U have multiple oxidation states that are readily accessible, and their f orbitals are extended and available for bonding.

Although there have been numerous reports of Ce and U exhibiting complex valent behavior in a variety of oxides, most of the evidence supporting these claims is indirect, such as the comparisons of lattice constants, color, or magnetic susceptibility data within a series. Whereas this information is useful qualitatively, a more quantitative perspective is essential if the subtleties of the charge distribution and its dynamics are to be understood fundamentally. Toward this end, we have chosen to investigate the details of electronic charge distribution in two compounds previously reported to have complex metal ion charge distributions, Ce_2MoO_6 and Ce_2UO_6.

Ce_2MoO_6 is a member of a series of compounds Ln_2MoO_6 (Ln = Y, La−Lu).[6] The assignment of formal oxidation states is straightforward for most of the compounds, i.e., Ln^{III} and Mo^{VI}. These compounds assume the color of the trivalent rare-earth ion and are poor conductors, as expected because the Mo^{VI}−O sublattice has no carriers. The exception to this behavior is Ce_2MoO_6, which is black. The black color has been previously used to support the argument that Ce transfers some of its charge to Mo, to form $Ce^{III}Ce^{IV}Mo^{V}O_6$.[6,7] This hypothesis was supported by magnetic susceptibility data and preliminary spectroscopic studies.[8] In addition to the unusual physical properties of Ce_2MoO_6 when compared with other members of the Ln_2MoO_6 series, the Ce analogue has also been reported to crystallize in the space group $Fm3m$[8] or in a supercell of the same space group,[6] a symmetry higher than the neighbouring La and Pr analogues, which are tetragonal.[9]

The solid-solution series $Ce_xU_{1-x}O_2$ forms from $Ce^{IV}O_2$ ($x = 1$) to $U^{IV}O_2$ ($x = 0$) with the same $Fm3m$ structure. The lattice constants, magnetic ordering temperatures, and effective moments have been measured as a function of x,[10] and anomalous behavior has been reported near the $x = {}^2/_3$ analogue, Ce_2UO_6. In addition, whereas CeO_2 is white and UO_2 is brown, the solid solutions with $x \approx 0.6$ are a deep blue color. These results have lead to the conclusion that there is charge transfer from Ce to U, either of the form

$$Ce_2^{IV}U^{IV}O_6 \leftrightarrow Ce_2^{III}U^{VI}O_6$$

which is suggested to be a dynamic process, or of the

[⊗] Abstract published in *Advance ACS Abstracts,* September 1, 1996.

(1) Varma, M. C. *Rev. Mod. Phys.* **1976**, *48*, 219−238.
(2) Lawrence, J. M.; den Boer, M. L.; Parks, R. D.; Smith, J. L. *Phys. Rev. B* **1984**, *29*, 568−575.
(3) Bornick, R. M.; Stacy, A. M. *Chem. Mater.* **1994**, *6*, 333.
(4) Netzer, F. P.; Bertel, E. In: *Handbook Phys. Chem. Rare Earths;* Gschneidner, K. A., Eyring, L., Eds.; North Holland: Amsterdam, 1982; Vol. 5, pp 217−320.
(5) Brazdil, J. F. In: *Characterization of Catalytic Materials*; Wachs, I. E., Fitzpatrick, L. E., Eds.; Butterworth-Heinemann: Boston, 1992; pp 47−68.
(6) Brixner, L. H.; Sleight, A. W.; Licis, M. S. *J. Solid State Chem.* **1972**, *5*, 186−190.
(7) Blasse, G. *J. Inorg. Nucl. Chem.* **1966**, *28*, 1488−1489.
(8) Manthiram, A.; Gopalakrishnan, J. *J. Less-Common Met.* **1984**, *99*, 107−111.
(9) Xue, J. S.; Antonio, M. R.; Soderholm, L. *Chem. Mater.* **1995**, *7*, 333−340.
(10) Hinatsu, Y.; Fujino, T. *J. Less-Common Met.* **1989**, *149*, 197−205.

S0897-4756(96)00208-6 CCC: $12.00

form

$$Ce_2^{IV}U^{IV}O_6 \rightarrow Ce_2^{III/IV}U^{IV/V}O_6$$

which is considered as a simple charge-transfer reaction that has not necessarily gone to completion.[10−14] Ce^{IV} is known to rapidly oxidize U^{IV} in solution,[15] supporting this hypothesis.

The initial objective of the work reported herein was to characterize quantitatively the charge distributions in Ce_2MoO_6 and Ce_2UO_6, including the dynamics of the transfer processes. The differences in bonding and reduction potentials between U and Mo in isostructural, high-symmetry environments were expected to aid in furthering the understanding of the subtle energetics and bonding requirements necessary to form intermediate or mixed-valent materials. X-ray absorption spectroscopy (XAS) was chosen for initial studies because it is a single-ion probe that is sensitive to the absorbing ion's oxidation state, and it is an established technique for investigating intermediate valence.[16] In addition, under favorable conditions the fast time scale of XAS (10^{-16} s) allows a study of the dynamics of the charge transfer. Unfortunately, we found no evidence, in any of our data on either of these compounds, for any charge transfer. All of our results showed *only* the presence of $Ce^{III}-Mo^{VI}$ and $Ce^{IV}-U^{IV}$, respectively. These results are presented in detail below. Preliminary results on Ce_2MoO_6 have been presented elsewhere.[17]

Experimental Section

Synthesis. Ce_2UO_6 was prepared according to standard procedures.[10] La_2MoO_6 and Tb_2MoO_6 were prepared from Ln_2O_3 and MoO_3 as described elsewhere;[9] Ce_2MoO_6 was made slightly differently because of the difficulty of obtaining Ce_2O_3. The compound was prepared by mixing the appropriate starting reagents according to

$$6CeO_2 + Mo + 2.05MoO_3 \rightarrow 3Ce_2MoO_6$$

MoO_3 was obtained from Cerac, and CeO_2 was a REacton product. These reagents were intimately mixed, sealed in a thick-walled quartz tube, and heated to 1200 °C. It was determined that a slight excess of MoO_3 was necessary to form a single-phase material; in its absence there were CeO_2 lines that appeared in the X-ray diffraction pattern. The necessity for excess MoO_3 is attributed to the fact that it sublimates at temperatures less than the reaction temperature of 1200 °C.[18] Four model compounds (MoO_3, $CaMoO_4$, La_2MoO_6, and Tb_2MoO_6) with structurally characterized molybdenum coordination environments were examined to facilitate comparisons with Ce_2MoO_6. The $CaMoO_4$ scheelite phase was prepared according to published procedures.[19]

Powder X-ray Diffraction. All samples were analyzed by powder X-ray diffraction, using a Scintag diffractometer equipped with a Cu tube, and operating in the $\theta-\theta$ mode with a flat-plate geometry. Except for Ce_2MoO_6, the data, and their analyses for cell constants, all agreed with published results. The powder pattern obtained from Ce_2MoO_6 was also consistent with published results,[6] including the presence of several very weak additional lines that could not be indexed on the simple fluorite, F-centered, cubic cell.

XAFS. Cerium L_3-edge and uranium $M_{4,5}$-edge XAFS data were obtained at ambient temperature with an electron-yield detector (The EXAFS Co.) on SSRL (Stanford Synchrotron Radiation Laboratory) wiggler beam line 4−1 using a 1 mm premonochromator slit and Si⟨111⟩ crystals. Mo $L_{2,3}$-edge XANES was collected with an electron-yield detector at ambient temperature on beam line X-19A at the NSLS (National Synchrotron Light Source) with a Si⟨111⟩ double-crystal monochromator.[20] Using a 2 mm (vertical) monochromator entrance slit provided an energy resolution of ca. 0.5 eV for the Mo L_3-edge energy.[20] This instrumental resolution is 3.6× smaller than the natural width of the L_3 core hole, 1.78 eV.[21] Therefore, the Mo L_3-edge XANES shown here is not obviously broadened by instrumental resolution effects. The L_3-edge region was scanned with a step size of 0.1 eV over the absorption resonances. Absolute energy calibration was set with the first absorption peak (2469.2 eV) in the S K-edge XANES for $Na_2S_2O_3 \cdot 5H_2O$.[22] Mo K-edge electron-yield XANES was collected at ambient temperature on beam line X-23A2 at the NSLS with a Si⟨311⟩ double-crystal monochromator and 1 mm (vertical) monochromator entrance slit. The approximate energy resolution at 20 keV was estimated to be about 5 eV, which is 10× larger than that for Mo L_3-edge XANES, and a little larger than the K-edge natural width, 4.52 eV.[21] These experimental conditions produce an unavoidable broadening (ca. 50%) of the primary data. The Mo K-edge and U L_3-edge transmission EXAFS were obtained at 10 K (Oxford Instruments CF1208 cryostat) on wiggler beam line 4−3 at the SSRL with a Si⟨220⟩ monochromator and 1 mm (vertical) premonochromator entrance slits. The EXAFS analysis was performed according to conventional methods[23,24] using the EXAFSPAK[25] computer programs.

Results

X-ray Powder Diffraction. The diffraction pattern shown in Figure 1 is not consistent with previous reports that Ce_2MoO_6 forms with the fluorite structure, in space group $Fm3m$.[8] Whereas the main diffraction lines have both positions and intensities consistent with the fluorite structure, there are also numerous very weak peaks, marked in the inset of Figure 1, that necessitate a larger unit cell, with lower symmetry. All the lines can be indexed using a P cubic cell, indicating that these are not impurity phase lines. In addition, neutron powder diffraction on the same sample reveals these lines to be much more intense, leading to the conclusion that they arise primarily from oxygen-superlattice ordering.[26]

(11) Hofmann, K. A.; Höschele, K. *Ber. Dtsch. Chem. Ges.* **1915**, *48*, 20−28.
(12) Rüdorff, W.; Valet, G. *Z. Anorg. Allg. Chem.* **1953**, *271*, 257−272.
(13) Brauer, V. G.; Tiessler, R. *Z. Anorg. Allg. Chem.* **1953**, *271*, 273.
(14) Robin, M. B.; Day, P. *Adv. Inorg. Chem. Radiochem.* **1967**, *10*, 247−422.
(15) Baker, F. W.; Newton, T. W.; Kahn, M. *J. Phys. Chem.* **1960**, *64*, 109.
(16) Rohler, J. In: *Handbook Phys. Chem. Rare Earths;* Gschneidner, K. A., Eyring, L., Hufner, S., Eds.; North Holland: Amsterdam, 1987; Vol. 16, pp 453−545.
(17) Antonio, M. R.; Xue, J. S.; Soderholm, L. *J. Alloys Compd.* **1994**, *207/208*, 444−448.
(18) Lide, D. R., Ed. *Handbook of Chemistry and Physics*, 76th ed.; Chemical Rubber Publishing Co.: Boca Raton, FL, 1995.
(19) Wandahl, G.; Christensen, A. N. *Acta Chem. Scand. Sect. A* **1987**, *41*, 358−360.
(20) Yang, C. Y.; Penner-Hahn, J. E.; Stefan, P. M. *Nucl. Instrum. Meth. Phys. Res., Sect. A* **1990**, *291*, 157−161.
(21) Krause, M. O.; Oliver, J. H. *J. Phys. Chem. Ref. Data* **1979**, *8*, 329−338.
(22) Song, I.; Rickett, B.; Janavicius, P.; Payer, J. H.; Antonio, M. R. *Nucl. Instrum. Meth. Phys. Res. A* **1995**, *360*, 634−641.
(23) Lytle, F. W. In: *Applications of Synchrotron Radiation;* Winick, H., et al., Eds.; Gordon and Breach: New York, 1989; Vol. 4, pp 135−223.
(24) Bertagnolli, H.; Ertel, T. S. *Angew. Chem., Int. Ed. Engl.* **1994**, *33*, 45−66.
(25) Pickering, I. J.; George, G. N. *Inorg. Chem.* **1995**, *34*, 3142−3152.
(26) Soderholm, L.; Antonio, M. R., unpublished.

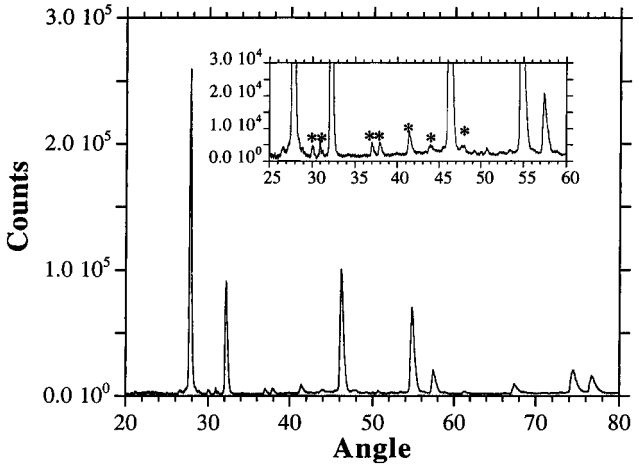

Figure 1. X-ray powder diffraction pattern of Ce_2MoO_6, taken with copper radiation. The most intense peaks can all be indexed in the $Fm3m$ space group, consistent with the CeO_2 structure. However, the weak peaks marked with asterisks in the inset are not consistent with this space group.

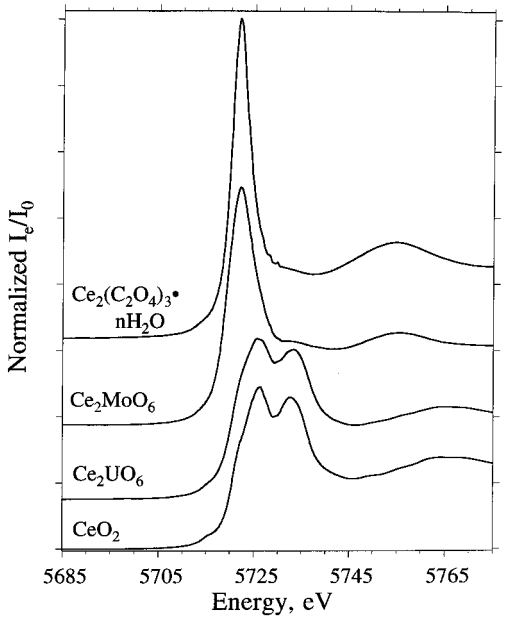

Figure 2. Ce L_3-edge, electron-yield XANES obtained at 295 K for Ce_2MoO_6, Ce_2UO_6, $Ce_2(C_2O_4)_3 \cdot nH_2O$ and CeO_2.

Ce XAFS. The valence of Ce is distinguishable by the X-ray absorption L_3-edge position and features[27] (XANES). Ce^{III} is evidenced by a single-line edge resonance, whereas Ce^{IV} produces a double-peaked resonance, with a peak separation of about 7.5 eV. The lower-energy peak of Ce^{IV} is shifted to about 4 eV to higher energy than the single resonance observed for Ce^{III}. It is apparent from Figure 2 that the Ce L_3-edge XANES obtained from Ce_2MoO_6 and Ce_2UO_6 are not the same. As previously reported,[17] Ce_2MoO_6 has a spectrum consistent with the presence of Ce^{III}. There is no evidence in the data for the presence of any Ce^{IV} or any intermediate-valence in this material. In sharp contrast, the double edge-resonance observed from Ce_2UO_6 is indicative of Ce^{IV}, as exemplified by CeO_2.[27] Whereas there is no evidence of the presence of any intermediate-valent Ce, a small charge transfer cannot be unambiguously ruled out in this case simply from the Ce L_3-edge XANES.

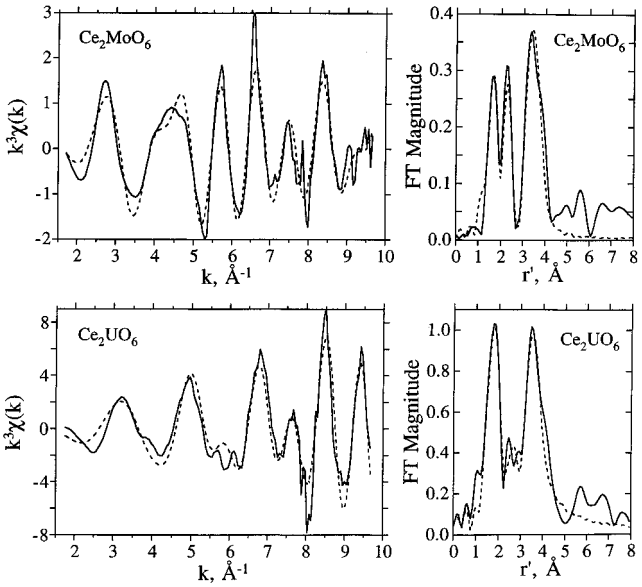

Figure 3. Left: Ce L_3-edge, electron-yield, $k^3\chi(k)$ EXAFS (295 K) for $Ce_2^{III}Mo^{VI}O_6$ and $Ce_2^{IV}U^{IV}O_6$. The best fits are shown as dashed lines. Right: Fourier transforms of the experimental (solid lines) and fitted (dashed lines) $k^3\chi(k)$ Ce EXAFS data of the left panel for Ce_2MoO_6 and Ce_2UO_6.

The different valences suggested for Ce in the molybdate versus the uranate are also discernible from the EXAFS data, despite the onset of the Ce L_2-edge at about 440 eV above the L_3-edge, which limits the resolution. The $k^3\chi(k)$ EXAFS and the corresponding Fourier transforms (FT) for Ce_2MoO_6 and Ce_2UO_6 are compared in Figure 3. It is clear from these data alone that the Ce^{III} coordination in Ce_2MoO_6 is different from the Ce^{IV} coordination in Ce_2UO_6. There are two well-resolved Ce−O interactions in Ce_2MoO_6, which, when fit to the $k^3\chi(k)$ EXAFS shown in Figure 3 (dashed lines), reveal 4 O at 2.31 Å and 4 O at 2.74 Å. This Ce coordination is *inconsistent* with the symmetry required for Ce in the $Fm3m$ space group previously assigned based on powder X-ray diffraction data.[8] In contrast, the oxygen coordination of Ce in Ce_2UO_6 (8 O at 2.29-(3) Å) is like that for CeO_2 (8 O at 2.343 Å), which has the fluorite, $Fm3m$ structure. The peaks observed in the FTs from both Ce_2MoO_6 and Ce_2UO_6 at about 3.4 Å (before phase shift correction) are attributed to Ce−M (M = Mo, U) interactions. The Ce−M backscattering was best fit with two terms: 2 Mo at 3.96(3) Å and 8 Ce at 3.91(3) Å for Ce_2MoO_6, and 4 U at 3.85(12) Å and 8 Ce at 3.81(4) Å for Ce_2UO_6. The results from the EXAFS analyses are summarized in Table 1.

Mo XAFS. The normalized Mo L_3-edge XANES data for the standards $CaMoO_4$ and La_2MoO_6 (Mo^{VI}; tetrahedral environment) and MoO_3 (Mo^{VI}; octahedral environment) are compared with the data from Ce_2MoO_6 in Figure 4. As shown in Table 2, the edge position of Mo in Ce_2MoO_6 is consistent with only the presence of hexavalent Mo. Mo^V has an edge-resonance energy that is shifted 2 eV to lower energy than observed for here for Mo^{VI},[28] and Mo^{IV} is shifted to even lower energies. Within the detection limits of these experiments of

(27) Antonio, M. R.; Soderholm, L. *Inorg. Chem.* **1994**, *33*, 5988−5993.

(28) de Groot, F. M. F.; Hu, Z. W.; Lopez, M. F.; Kaindl, G.; Guillot, F.; Tronc, M. *J. Chem. Phys.* **1994**, *101*, 6570−6576.

Table 1. Curve-Fitting Results for the Unfiltered $k^3\chi(k)$ EXAFS Data of CeO_2, UO_2, Ce_2UO_6, and Ce_2MoO_6 Shown in Figures 3, 5, and 7[a]

		oxygen		cerium		uranium		molybdenum	
cmpd	edge	*N*	*r*, Å	*N*	*r*, Å	*N*	*r*, Å	*N*	*r*, Å
CeO_2[b]	Ce L_3	8	2.35(1)	12	3.82(1)				
UO_2[c]	U L_3	8	2.34(3)			12	3.86(1)		
Ce_2UO_6	Ce L_3	8	2.29(3)	8	3.81(4)	4	3.85(12)		
	U L_3	8	2.33(1)	8	3.84(1)	4	3.90(2)		
Ce_2MoO_6	Ce L_3	4	2.31(5)	8	3.91(3)			2	3.96(3)
		4	2.74(3)						
	Mo K	4	1.79(1)	2	4.00(4)			1	3.88(3)

[a] All curve fitting was performed using single-scattering theoretical phase and amplitude functions obtained from FEFF 6.01a; see: Rehr, J. J.; Mustre de Leon, J.; Zabinsky, S. I.; Albers, R. C. *J. Am. Chem. Soc.* **1991**, *113*, 5135−5140. Mustre de Leon, J.; Rehr, J. J.; Zabinsky, S. I.; Albers, R. C. *Phys. Rev. B: Condens. Matter* **1991**, *44*, 4146−4156. Coordination numbers, *N*, were refined using best integer fits, see: George, G. N.; Pickering, I. J. *EXAFSPAK: A Suite of Computer Programs for Analysis of X-ray Absorption Spectra*; 1995; pp 50−51. The estimated error for all values of *N* is ± 20%. Even for the short Ce L_3-edge EXAFS data with $\Delta k = 8$ Å^{-1} and $\Delta r = 3$ Å, the number of curve fitting parameters (8−12) was always less than the number of independent data points, $N_{idp} = 2\Delta k\Delta r/\pi = 15$. The numbers in parentheses represent the estimated 95% confidence limits (3σ) obtained from the diagonal elements of the covariance matrix of the least-squares fit. [b] Crystallographic values are 8 O at 2.343 Å and 12 Ce at 3.826 Å. The $k^3\chi(k)$ EXAFS data and fit for CeO_2 are available as supporting information. [c] Crystallographic values are 8 O at 2.363 Å and 12 U at 3.859 Å. The $k^3\chi(k)$ EXAFS data and fit for UO_2 are available as supporting information.

Table 2. Mo L_3-Edge XANES Peak Positions and Intensities for the Normalized, Electron-Yield Data of Figure 4 as Well as the Principal Inflection Point (IP) Energies of the First Differential XANES[a]

	first peak			second peak			10*Dq*		
sample	IP,[b] eV	posn, eV	inten	IP,[b] eV	posn, eV	inten	primary	fst diff	snd diff[c]
$CaMoO_4$	2522.6	2523.4	5.16	2524.8	2525.5	8.79	2.1	2.2	2.3
MoO_3	2522.8	2523.6	7.63	2525.7	2526.4	6.17	2.8	2.9	3.4
La_2MoO_6	2522.5	2523.3	5.26	2524.6	2525.3	7.76	2.0	2.1	2.3
Ce_2MoO_6	2522.5	2523.4	5.63	2524.7	2525.3	6.83	1.9	2.2	2.2
Tb_2MoO_6	2522.4	2523.3	5.70	2524.5	2525.3	7.25	2.0	2.1	2.1/3.5[d]

[a] Also tabulated are the approximate values of 10*Dq* obtained from the peak separation in the primary, first differential, and second differential Mo L_3-edge XANES. Comparison of the tabulated energies for the three lanthanide molybdates, Ln_2MoO_6, reveals that they are the same within the average experimental error, ±0.2 eV. [b] Inflection point energies from first differential Mo L_3-edge XANES. [c] Peak splitting obtained from the second differential Mo L_3-edge XANES as in ref 33. [d] The coordination of Mo^{VI} in Tb_2MoO_6 is unusual. It consists of a distorted tetrahedron of O atoms at an average distance of 1.803 Å with a distant O atom at 2.214 Å to form an irregular square pyramid.[9]

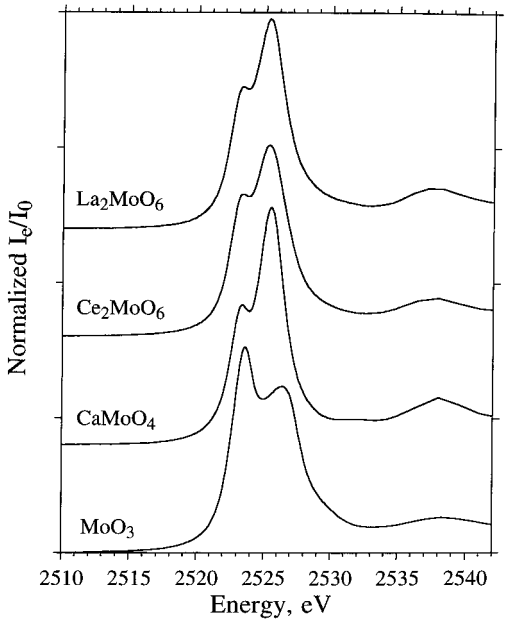

Figure 4. Mo L_3-edge, electron-yield XANES obtained at 295 K for $CaMoO_4$, MoO_3, La_2MoO_6, and Ce_2MoO_6.

about 5%, we conclude that there is only Mo^{VI} in Ce_2MoO_6. Our Mo K-edge XANES, available as supporting information, also supports this interpretation.

The double-peak structures observed in the Mo L_3-edge XANES data presented in Figure 4 are caused by crystal-field splitting of the 4d orbitals.[28−33] These splittings provide an approximate value of the crystal field strength parameter, 10*Dq*,[34−41] the magnitude of which is diagnostic of the coordination environment. Typical splittings for Mo^{VI} have been reported to be 1.8−2.4 eV for tetrahedral coordination and 2.8−4.5 eV for octahedral coordination.[33] Table 2 contains the peak splittings (in electronvolts) obtained from the normalized Mo XANES and from the first and second differential XANES. The splittings obtained from our standards,

(29) Hedman, B.; Penner-Hahn, J. E.; Hodgson, K. O. In: *EXAFS and Near Edge Structure III;* Hodgson, K. O., Hedman, B., Penner-Hahn, J. E., Eds.; Springer-Verlag: Berlin 1984; pp 64−66.
(30) Hedman, B.; Frank, P.; Gheller, S. F.; Roe, A. L.; Newton, W. E.; Hodgson, K. O. *J. Am. Chem. Soc.* **1988**, *110*, 3798−3805.
(31) George, G. N.; Cleland, W. E., Jr.,; Enemark, J. H.; Smith, B. E.; Kipke, C. A.; Roberts, S. A.; Cramer, S. P. *J. Am. Chem. Soc.* **1990**, *112*, 2541−2548.
(32) Evans, J.; Mosselmans, J. F. W. *J. Phys. Chem.* **1991**, *95*, 9673−9676.
(33) Bare, S. R.; Mitchell, G. E.; Maj, J. J.; Vrieland, G. E.; Gland, J. L. *J. Phys. Chem.* **1993**, *97*, 6048−6053.
(34) George, S. J.; van Elp, J.; Chen, J.; Ma, Y.; Chen, C. T.; Park, J. B.; Adams, M. W. W.; Searle, G. B.; de Groot, F. M. F.; Fuggle, J. C.; Cramer, S. P. *J. Am. Chem. Soc.* **1992**, *114*, 4426−4427.
(35) dit Moulin, C. C.; Rudolf, P.; Flank, A. M.; Chen, C. T. *J. Phys. Chem.* **1992**, *96*, 6196−6198.
(36) Abbate, M.; de Groot, F. M. F.; Fuggle, J. C.; Fujimori, A.; Sawatzky, G. A.; Takano, M. Takeda, Y.; Eisaki, H.; Uchida, S. *Phys. Rev B: Condens. Matter* **1992**, *46*, 4511−4519.
(37) de Groot, F. M. F.; Fuggle, J. C.; Thole, B. T.; Sawatzky, G. A. *Phys. Rev. B: Condens. Matter* **1990**, *42*, 5459−5468.
(38) de Groot, F. M. F.; Fuggle, J. C.; Thole, B. T.; Sawatzky, G. A. *Phys. Rev. B: Condens. Matter* **1990**, *41*, 928−937.
(39) Brydson, R.; Garvie, L. A. J.; Craven, A. J.; Sauer, H.; Hofer, F.; Cressey, G. *J. Phys.: Condens. Matter* **1993**, *5*, 9379−9392.
(40) van der Laan, G.; Kirkman, I. W. *J. Phys.: Condens. Matter* **1992**, *4*, 4189−4204.
(41) Choy, J.-H.; Kim, D.-K.; Demazeau, G.; Jung, D.-Y. *J. Phys. Chem.* **1994**, *98*, 6258−6262.

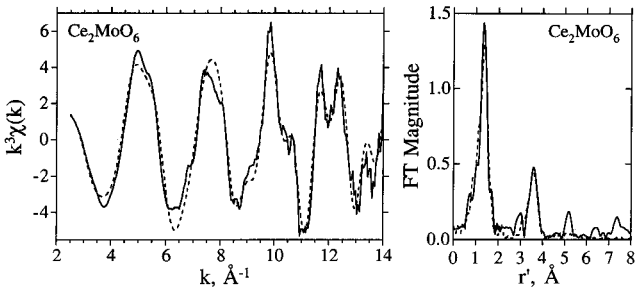

Figure 5. Left: Transmission $k^3\chi(k)$ EXAFS (10 K) for the Mo K-edge of $Ce_2^{III}Mo^{VI}O_6$. The best fit is shown as the dashed line. Right: Fourier transform of the experimental (solid line) and fitted (dashed line) $k^3\chi(k)$ Mo EXAFS of the left panel for Ce_2MoO_6.

shown in Table 2, are within the ranges reported for their coordination environments. For Ce_2MoO_6, the splitting of the L_3-edge resonance is 2.2 eV and is consistent with a four-coordinate, tetrahedral-like oxygen environment about molybdenum(VI).

Supporting evidence for this molybdenum stereochemistry in Ce_2MoO_6 is provided by the relative intensities of the Mo L_3 edge resonances. For a tetrahedral Mo environment, such as in $CaMoO_4$ and La_2MoO_6, the leading resonance is less intense than the second one,[33] as demonstrated in Figure 4. For MoO_3 with a distorted octahedral Mo environment, there is a reversal of intensities, such that the leading resonance is the more intense. From simple ligand field theory concepts, these relative intensity differences correlate with the hole count of the empty electronic states. The relative edge-resonance intensities for Ce_2MoO_6 are more like those for $CaMoO_4$ and La_2MoO_6 than for MoO_3. This result provides strong support for the conclusion that Mo^{VI} is centered in a tetrahedral-like coordination of oxygen atoms in Ce_2MoO_6.

A more quantitative description of the immediate coordination of Mo^{VI} in Ce_2MoO_6 is provided through analysis of the Mo K-edge $k^3\chi(k)$ EXAFS, which is shown in Figure 5. The corresponding FT reveals a single intense peak, which is due to oxygen backscattering. Distant peaks beyond ca. 3.5 Å, due to Mo−M (M = Ce, Mo) interactions, are weak yet clearly visible. The Mo $k^3\chi(k)$ EXAFS was modeled with three components, as reported in Table 1. The Mo−O interatomic distance of 1.79(1) Å is typical of Mo^{VI}−O bonds in compounds with tetrahedral coordination.[42−44] The independently refined Mo−Ce and Ce−Mo distances from the Mo and Ce EXAFS analyses, respectively, are all consistent. The EXAFS-determined metrical parameters for Ce_2MoO_6 provide confirming evidence of the XANES, for Mo^{VI} in a tetrahedral-like environment.

U XAFS. U L_3- and M_5-edge X-ray absorption data have been combined to reveal clearly interpretable differences between U^{IV}, U^{V}, and U^{VI} oxidation states and their coordination environments.[45−53] The U L_3-

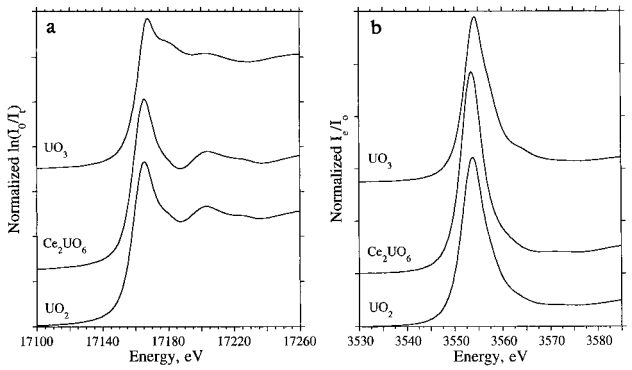

Figure 6. (a) U L_3-edge, transmission XANES obtained at 10 K for Ce_2UO_6, UO_3, and UO_2. (b) U M_5-edge, electron-yield XANES obtained at 295 K for Ce_2UO_6, UO_3, and UO_2.

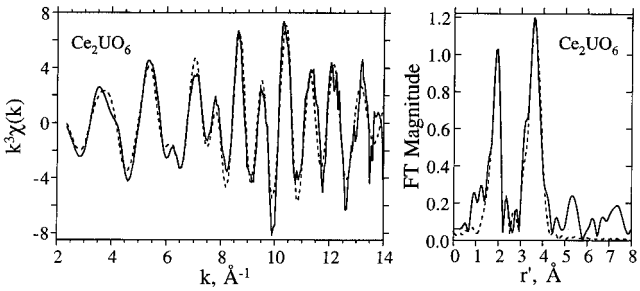

Figure 7. Left: Transmission $k^3\chi(k)$ EXAFS (10 K) for the U L_3-edge of $Ce_2^{IV}U^{IV}O_6$. The best fit is shown as a dashed line. Right: Fourier transforms of the experimental (solid line) and fitted (dashed line) $k^3\chi(k)$ U EXAFS data of Ce_2UO_6.

and M_5-edge XANES for Ce_2UO_6, UO_2, and UO_3 are shown in Figure 6a, b. The L_3-edge peaks for $U^{IV}O_2$ and Ce_2UO_6 are similar and ca. 2 eV below the L_3-edge peak for $U^{VI}O_3$. This edge shift is consistent with the with presence of U^{IV} in Ce_2UO_6. Likewise, the M_5-edge resonance for Ce_2UO_6 is ca. 1 eV below the corresponding resonance for UO_3. This, too, is consistent with the presence of U^{IV} in Ce_2UO_6. There is no evidence in the XANES data for any U^{V} or U^{VI}, contrary to expectations based on previous reports.[10−12,14,54]

The U L_3-edge $k^3\chi(k)$ EXAFS and the corresponding FT data are shown in Figure 7. Uranium(IV) is coordinated to 8 O atoms at 2.33(1) Å, and the distant U−M interactions, visible in the FT data at ca. 3.5 Å (before phase shift correction), were modeled by fitting with 8 Ce at 3.84(1) Å and 4 U at 3.90(2) Å. The U−O and U−M metrical data obtained from the U L_3-edge EXAFS (Table 1) are in agreement with the corresponding Ce−O and Ce−M parameters obtained independently from the Ce L_3-edge EXAFS.

(42) Jeitschko, W.; Sleight, A. W.; McClellan, W. R.; Weiher, J. F. *Acta Crystallogr.* **1976**, *B32*, 1163−1170.
(43) Abrahams, S. C.; Reddy, J. M. *J. Chem. Phys.* **1965**, *43*, 2533−2543.
(44) Smith, G. W.; Ibers, J. A. *Acta Crystallogr.* **1965**, *B19*, 269−275.
(45) Kalkowski, G.; Kaindl, G.; Bertram, S.; Schmiester, G.; Rebizant, J.; Spirlet, J. C.; Vogt, O. *Solid State Commun.* **1987**, *64*, 193−196.
(46) Kalkowski, G.; Kaindl, G.; Brewer, W. D.; Krone, W. *Phys. Rev. B* **1987**, *35*, 2667−2677.
(47) Petiau, J.; Calas, G.; Petitmaire, D.; Bianconi, A.; Benfatto, M.; Marcelli, A. *Phys. Rev. B* **1986**, *34*, 7350−7361.
(48) Farges, F.; Ponader, C. W.; Calas, G.; Brown, G. E., Jr. *Geochim. Cosmochim. Acta* **1992**, *56*, 4205−4220.
(49) Francis, A. J.; Dodge, C. J.; Lu, F.; Halada, G. P.; Clayton, C. R. *Environ. Sci. Technol.* **1994**, *28*, 636−639.
(50) Bertsch, P. M.; Hunter, D. B.; Sutton, S. R.; Bajt, S.; Rivers, M. L. *Environ. Sci. Technol.* **1994**, *28*, 980−984.
(51) Greaves, G. N.; Barrett, N. T.; Antonini, G. M.; Thornley, F. R.; Willis, B. T. M.; Steel, A. *J. Am. Chem. Soc.* **1989**, *111*, 4313−4324.
(52) Berry, F. J.; Murray, A.; Steel, A. T. *J. Chem. Soc., Faraday Trans. 1* **1988**, *84*, 2783−2793.
(53) Chisholm-Brause, C.; Conradson, S. D.; Buscher, C. T.; Eller, P. G.; Morris, D. E. *Geochim. Cosmochim. Acta* **1994**, *58*, 3625−3631.
(54) Brauer, G.; Tiessler, R. *Z. Anorg. Allg. Chem.* **1953**, *271*, 273−280.

Discussion

Our X-ray powder diffraction patterns clearly demonstrate that Ce_2UO_6 and Ce_2MoO_6 are not isostructural. All the diffraction peaks observed from Ce_2UO_6 are indexable in the *Fm*3*m* space group, and the structure appears consistent with the same fluorite structure exhibited by both CeO_2 and UO_2. This result is consistent with a variety of other reports that the series $Ce_xU_{1-x}O_2$ exists for all values of x.[10,55] In contrast, the X-ray diffraction pattern observed for Ce_2MoO_6 is inconsistent with that expected from a fluorite structure. Whereas the major diffraction peaks are indeed indexable in an F-centered cubic cell, the presence of weak additional lines rule out this symmetry. These lines have been previously observed and have been attributed to superlattice lines because they can be indexed on a cubic supercell, although the strict systematic absence requirements for *Fm*3*m* are violated. A comparison of the X-ray results with neutron diffraction data from the same material reveals that most of the extra lines have much more intensity in the neutron data, with some of these lines actually approaching the intensity of the fluorite lines.[26] The X-ray and neutron data taken together demonstrate that the metal ions are arranged in an essentially fluorite-like lattice but that the oxygen atoms destroy the pure *Fm*3*m* symmetry.

From the arguments presented above, we conclude that Ce_2UO_6 and Ce_2MoO_6 are not isostructural, as assumed initially. Nevertheless, it would have remained of interest to characterize any intermediate-valent behavior in these systems. Unfortunately, the XANES data show no indication of intermediate or mixed valence in either material. X-ray absorption experiments have a characteristic time scale of about 10^{-16} s, which is much faster than any dynamic charge-transfer processes. When it does occur, the appearance of intermediate valence is clearly discernible by XANES.[16]

The XANES unequivocally show that both Ce and U are tetravalent. The Ce and U EXAFS from Ce_2UO_6 support the structural conclusions from the diffraction data. The EXAFS obtained from Ce and U are similar to each other, as shown in Figures 3 and 7, and both are consistent with the metals coordinated to 8 oxygens at 2.3 Å. Best integers fits of the Ce and U EXAFS show that the metal-atom coordinations are best represented as 8 Ce and 4 U. This fit agrees with the metal-atom coordination predicted from a binomial analysis of coordination probabilities based on a statistical distribution of Ce and U in the material. This result supports the argument that Ce_2UO_6 is a solid solution, in which the Ce and U atoms are disordered on the same cation site in the *Fm*3*m* structure.

It has been previously argued whether or not Ce_2UO_6 is a definite compound or a member of the solid-solution series $Ce_xU_{1-x}O_2$.[10,11,14,55] The suggestion that a metal-ion stoichiometry near 2:1 is somehow special arose from the anomalous color observed for materials near this stoichiometry and has been supported by magnetic susceptibility data. Whereas UO_2 is brown and CeO_2 is white, their solid solutions in the range of a 2:1 stoichiometry are deep blue.[55] The blue color was argued to arise from the charge transfer

$$Ce_2^{IV}U^{IV}O_6 \leftrightarrow Ce_2^{III}U^{VI}O_6$$ [8,10,11]

in which U^{IV} is a powerful enough reductant to fully reduce Ce to trivalent. It has also been argued that at the 2:1 stoichiometry the color should be at its *minimum* because intermediate-valent Ce or U concentrations would be at their minimum.[14] In other words, the lowest probability of either a Ce^{III} to Ce^{IV} or U^{IV} to U^{VI} optical transition would occur exactly at the metal-ion ratio that corresponds to Ce_2UO_6. Consequently, it was proposed that the blue color arises from a charge transfer of the form

$$Ce_2^{IV}U^{IV}O_6 \leftrightarrow Ce^{III}Ce^{IV}U^{V}O_6$$ [14]

in which not all the Ce is reduced. This reaction would result in an intermediate-valent Ce ion.

In addition to the dark color observed for samples with a Ce:U ratio near to 2:1, the effective moments, determined by a simple Curie−Weiss analysis of $Ce_xU_{1-x}O_2$ susceptibility data, are seen to change as a function of x, reaching a broad maximum near $x = 0.6$.[10] The concentration dependence of the effective moment in the $Ce_xU_{1-x}O_2$ series has again been attributed to an in situ oxidation of U by Ce.[10] The fact that similar behavior is not observed in the corresponding $Th_xU_{1-x}O_2$[56] in which the Th is unambiguously tetravalent over the entire concentration range is used to support the argument.

The results presented herein demonstrate that there is no significant charge transfer between the metal ions. Both Ce and U are essentially tetravalent. The similarity in the ionic radii of tetravalent Ce and U, they differ by about 3%, is consistent with a disordering of these two ions on a single crystallographic site. A mixture of Ce^{III} and U^{VI} would have necessitated a disordering between ions with ionic radii that differ by more than 30%.[57] The absence of any significant charge transfer, which has been argued to preferentially stabilize the 2:1 metal-ion stoichiometry, weakens the argument that the 2:1 Ce to U stoichiometry can be distinguished from the rest of the $Ce_xU_{1-x}O_2$ solid-solution series.

These results contradict the fundamental argument that significant Ce−U charge transfer is responsible for the unusual color, resistivity, and magnetic susceptibility observed for Ce_2UO_6 relative to the end members of the $Ce_xU_{1-x}O_2$ series, and suggests to us another alternative. We propose that the energetics of this series permits significant bonding, or hybridization, involving Ce, U, and O orbitals, that is optimized at intermediate values of x. This bonding involves *no charge transfer* but would instead be strictly covalent in nature. The strength of bonding interactions is known to depend on the degree of orbital overlap, coincidence of energetics of localized orbitals, and the orbital symmetries.[58] Ce, the lightest lanthanide with f-orbital occupation, has radially extended f orbitals that are available for bonding. Bonding would result in the

(55) Magneli, A.; Kihlborg, L. *Acta Chem. Scand.* **1951**, *5*, 578−580.

(56) Hinatsu, Y.; Fujino, T. *J. Solid State Chem.* **1985**, *60*, 195−205.

(57) Shannon, R. D.; Prewitt, C. T. *Acta Crystallogr. Sect. B* **1969**, *25*, 925−945.

(58) Albright, T. A.; Burdett, J. K.; Whangbo, M.-H. *Orbital Interaction in Chemistry*; Wiley: New York, 1985, p 447.

formation of f-band states, perhaps involving some oxygen p character. The stabilization energy of these bands may well result in a bandgap that could account for both the color and resistivity behavior. In addition, significantly increased bonding may result in somewhat itinerant f electrons, which would add an additional Pauli paramagnetic term to the susceptibility. This temperature-independent term would change the effective moment determined from the data[10] unless it is included in the analysis. Whereas all the data presented here are consistent with the proposed bonding effects, electronic calculations are necessary to confirm this hypothesis.

The XANES results obtained from Ce_2MoO_6 are irrefutable. Ce is trivalent and Mo is hexavalent to within the detection limit of our experiment, which is estimated to be about 5%. We found no evidence for the presence of pentavalent Mo previously reported from XANES data obtained from the Mo K-edge (using a bent-crystal X-ray spectrograph)[8,59] despite the fact that the material examined here was prepared in the same manner and showed the same "fluorite-based" lattice constant as the material previously examined. There is no evidence for any charge transfer, either dynamic or static, or any intermediate valence. The large size difference between Ce^{III} and Mo^{VI}, as well as their different expected coordination environments are consistent with the cation ordering observed from the EXAFS results reported herein. The determination of a tetrahedral coordination about Mo is consistent with the known structural chemistry of Mo^{VI}.

In sharp contrast to the results on Ce_2UO_6, the Ce and Mo EXAFS from Ce_2MoO_6 look very different from each other, as well as from those obtained from the corresponding uranate. The Ce is located in a distorted, 8-coordinate environment, whereas the molybdenum is 4-coordinate and the coordination is closely depicted as tetrahedral. The EXAFS data provide further evidence that Ce_2MoO_6 does not have the Ce−Mo cation disorder necessary for the fluorite-structure type. This absence of cation disorder is not surprising when it is considered that site disordering usually occurs between two ions that prefer similar coordination environments and whose ionic radii do not differ by more than about 15%. Such would not be the case for Ce and Mo in Ce_2MoO_6, irrespective of their oxidation states. These data directly support the X-ray and neutron diffraction findings for this material, and taken all together, these results constitute conclusive evidence that the cations order in Ce_2MoO_6 and that the simple fluorite, $Fm3m$ structure does not adequately describe the structure of this material. Furthermore, these results are not inconsistent with the magnetic susceptibility previously reported for this material.[8,17] The nonlinearity of a simple Curie plot renders problematic any effective moment analysis of the cation valence in this case.[17]

The description of Ce_2MoO_6 outlined herein with trivalent cerium and hexavalent molybdenum is inconsistent with previously proposed charge-transfer models.[6,8,60] These results clearly demonstrate that the reduction of Mo^{VI} by Ce^{III} does not occur to any appreciable extent and is not responsible for the unusual structure, color, or electronic properties of this material. Again we suggest, as we did for the Ce_2UO_6 material, that there may be significant bonding (or hybridization) involving Ce, Mo, and O orbitals. This bonding may stabilize the oxygen stoichiometry and help to explain why it has not been possible to make oxygen deficient compositions such as $Ce_2MoO_{5.5}$[26] or Ce_2MoO_5.[61−63] Although these grossly oxygen-deficient materials cannot be prepared, a slight nonstoichiometry, like 1 part in 10^3, may be enough to make this material black and semiconducting. The effect on the cation valences caused by an oxygen deficiency of this small magnitude is beyond the limits of detection of the XAFS techniques employed here.

The present results lead to a quandary about the structure of Ce_2MoO_6. With a Ce^{III} and Mo^{VI} cation distribution, it is difficult to rationalize its apparently unique structure. The other $Ln_2^{III}M^{VI}O_6$ compounds (i.e., Ln ≡ La, Pr, Nd, Sm−Lu) crystallize in two structural modifications: (1) a monoclinic (α) form with $Ln-O_8$ and $Mo-O_5$ coordination, as illustrated by α-Sm_2MoO_6[64] and α-Tb_2MoO_6,[9] and (2) a tetragonal (γ) form with $Ln-O_8$ and $Mo-O_4$ coordination, such as found for γ-La_2MoO_6[9] and γ-Nd_2MoO_6.[65] Ce_2MoO_6 is the archetypal example of a third type of structural modification, which is designated the β structure. It is thought to be a cubic transitional form with an unknown fluorite-like structure and unknown Ln and Mo coordination.[64] The EXAFS results reported here revealed a distorted $Ce-O_8$ coordination environment with 4 O atoms at 2.31(5) Å and 4 O atoms at 2.74(3) Å. This coordination is typical for $La^{III}-Nd^{III}$, such as found for La^{III} in γ-La_2MoO_6 (4 O at 2.394 Å and 4 O at 2.712 Å[9]) and Nd^{III} in γ-Nd_2MoO_6 (4 O at 2.33 Å and 4 O at 2.65 Å[65]) as well as Ce^{III} and La^{III} in the perovskites $CeTiO_3$ and $LaTiO_3$ (4 O at 2.47 Å and 4 O at 2.73 Å[66,67]). Whereas Ce^{IV} is also typically 8-fold coordinated by oxygen, the coordination polyhedra are less distorted and the average $Ce^{IV}-O$ interatomic distance (2.33−2.36 Å)[68] is substantially less than that for $Ce^{III}-O$. For example, the average $Ce-O_8$ distances in $Ce^{III}NbO_4$, A-Ce_2O_3, and $Ce^{III}TaO_4$, are 2.480, 2.505, and 2.520 Å, respectively.[69,70] The observation of distant Mo−M interactions in the FT data (Figure 5) suggests that the cation distribution about Mo^{VI} in Ce_2MoO_6 is better ordered than that for Tb_2MoO_6 and probably similar to that for La_2MoO_6.[9]

Insofar as metal oxidation states and structural environments dictate a wide range of catalytic behavior for bulk metal oxides,[5] the remarkable differences

(59) Manthiram, A.; Sarode, P. R.; Madhusudan, W. H.; Gopalakrishnan, J.; Rao, C. N. R. *J. Phys. Chem.* **1980**, *84*, 2200−2203.
(60) Brixner, L. H. *Rev. Chim. Mineral.* **1973**, *10*, 47−61.
(61) Manthiram, A.; Gopalakrishnan, J. *J. Less-Common Met.* **1979**, *68*, 167−174.
(62) Manthiram, A.; Gopalakrishnan, J. *Proc. Indian Acad. Sci.* **1978**, *87A*, 267−273.
(63) Kerner-Czeskleba, H.; Tourne, G. *Mater. Res. Bull.* **1978**, *13*, 271−278.
(64) Klevtsov, V. P.; Kharchenko, L. Y.; Klevtsova, R. F. *Sov. Phys. Crystallogr.* **1975**, *20*, 349−353.
(65) Efremov, V. A.; Tyulin, A. V.; Trunov, V. K. *Sov. J. Coord. Chem., Engl. Trans.* **1987**, *13*, 721−727.
(66) Eitel, M.; Greedan, J. E.; *J. Less-Common Met.* **1986**, *116*, 95−104.
(67) Goral, J. P.; Greedan, J. E. *J. Magn. Magn. Mater.* **1983**, *37*, 315−321.
(68) Lindgren, O. *Acta. Chem. Scand., Sect. A* **1977**, *31*, 453−456.
(69) Bärnighausen, H.; Schiller, G. *J. Less-Common Met.* **1985**, *110*, 385−390.
(70) Santoro, A.; Marezio, M.; Roth, R. S.; Minor, D. *J. Solid State Chem.* **1980**, *35*, 167−175.

between the solid-state properties of Ce_2MoO_6 and Ce_2UO_6 suggest the possibility of different catalytic behavior. There are a number of industrially important partial oxidation process that use bismuth molybdate based catalysts, such as Bi_2MoO_6.[5,71−78] We wonder what the effects of bismuth(III) doping of Ce_2MoO_6 to form $Ce_{2-x}Bi_xMoO_6$ might have upon the cation valence and coordination and, ultimately, the possible catalytic properties. Furthermore, we feel that in situ XAFS investigations of Ce_2MO_6 under oxidizing conditions might reveal the formation of $U^{V,VI}$ sites in $Ce_2^{IV}U^{IV}O_6$ and Ce^{IV} sites in $Ce_2^{III}Mo^{VI}O_6$. Likewise, under reducing conditions, it may be possible to form Ce^{III} sites in Ce_2UO_6 and $Mo^{IV,V}$ sites in Ce_2MoO_6. We hope that this report will stimulate catalytic studies of Ce_2MoO_6 and also its crystal structure solution and refinement.

(71) Burban, P. M.; Schuit, G. C. A.; Koch, T. A.; Bischoff, K. B. *J. Catal.* **1990**, *126*, 317−325.
(72) Burban, P. M.; Schuit, G. C. A.; Koch, T. A.; Bischoff, K. B. *J. Catal.* **1990**, *126*, 326−338.
(73) Brazdil, J. F.; Suresh, D. D.; Grasselli, R. K. *J. Catal.* **1980**, *66*, 347−367.
(74) Carson, D.; Coudurier, G.; Forissier, M. Vedrine, J. C.; Laarif, A.; Theobald, F. *J. Chem. Soc., Faraday Trans. 1* **1983**, *79*, 1921−1929.
(75) Grasselli, R. K.; Burrington, J. D.; Brazdil, J. F. *Faraday Discuss. Chem. Soc.* **1982**, *72*, 203−223.
(76) Batist, P. A.; Bouwens, J. F. H.; Schuit, G. C. A. *J. Catal.* **1972**, *25*, 1−11.
(77) Matsuura, I.; Schut, R.; Hirakawa, K. *J. Catal.* **1980**, *63*, 152−166.
(78) Snyder, T. P. Hill, C. G., Jr. *Catal. Rev.—Sci. Eng.* **1989**, *31*, 43−95.

Acknowledgment. We thank Drs. Graham George (SSRL) and Lars Furenlid (NSLS) for assistance with the XAFS measurements. The NSLS is supported by the U.S. Department of Energy, Division of Material Sciences, and Division of Chemical Sciences. The SSRL is operated by the Department of Energy, Office of Basic Energy Sciences. The SSRL Biotechnology Program is supported by the NIH, Biomedical Resource Technology Program, Division of Research Resources and by the Department of Energy, Office of Health and Environmental Research. The work reported herein was supported by the U.S. DOE, Basic Energy Sciences—Chemical Sciences, under contract No. W-31-109-ENG-38.

Supporting Information Available: Ce and U L_3-edge $k^3\chi(k)$ EXAFS data and curve-fitting results as well as Fourier transform data for CeO_2 and UO_2 (2 pages). Ordering information is given on any current masthead page.

CM960208C